AWARD NUMBER: W81XWH-13-1-0439

TITLE: Alpha2-Adrenergic Receptors and Breast Tumor Stroma: A Novel Pathway Driving Breast Cancer Growth and Metastasis

PRINCIPAL INVESTIGATOR: Kelley S. Madden, PhD

CONTRACTING ORGANIZATION: University of Rochester
Rochester, NY 14611-3847

REPORT DATE: October 2015

TYPE OF REPORT: Annual

PREPARED FOR: U.S. Army Medical Research and Materiel Command
Fort Detrick, Maryland 21702-5012

REPORT DOCUMENTATION PAGE

Form Approved
OMB No. 0704-0188

1. REPORT DATE	2. REPORT TYPE	3. DATES COVERED
October 2015	Annual	30 Sep 2014 - 29 Sep 2015

4. TITLE AND SUBTITLE

Alpha2-Adrenergic Receptors and Breast Tumor Stroma: A Novel Pathway Driving Breast Cancer Growth and Metastasis

5a. CONTRACT NUMBER

5b. GRANT NUMBER
W81XWH-13-1-0439

5c. PROGRAM ELEMENT NUMBER

6. AUTHOR(S)

Kelley S. Madden, PhD

E-Mail: Kelley_Madden@urmc.rochester.edu

5d. PROJECT NUMBER

5e. TASK NUMBER

5f. WORK UNIT NUMBER

7. PERFORMING ORGANIZATION NAME(S) AND ADDRESS(ES)

University of Rochester
910 Genesee St. Ste. 200
Rochester, NY 14611-3847ß

8. PERFORMING ORGANIZATION REPORT NUMBER

9. SPONSORING / MONITORING AGENCY NAME(S) AND ADDRESS(ES)

U.S. Army Medical Research and Materiel Command
Fort Detrick, Maryland 21702-5012

10. SPONSOR/MONITOR'S ACRONYM(S)
U.S. Army Medical Research and Materiel Command Fort Detrick, Maryland 21702-5012

11. SPONSOR/MONITOR'S REPORT NUMBER(S)

12. DISTRIBUTION / AVAILABILITY STATEMENT

Approved for Public Release; Distribution Unlimited

13. SUPPLEMENTARY NOTES

14. ABSTRACT

Breast cancer metastasis is driven by sympathetic nervous system (SNS) and ß-adrenergic receptor (ß-AR) activation, but the role for α2-AR, a major class of SNS receptors, has not been elucidated. The goal of this proposal is to characterize the effects of dexmedetomidine (DEX), a highly selective α2-AR agonist, on tumor metastasis in preclinical models of breast cancer. Using EO771, a metastatic mammary adenocarcinoma in C57BL/6/c mice, α2-AR activation increased tumor growth, but not metastasis to the lungs. In C57BL/6 mice treated with a ß2-AR-selective agonist, EO771 tumor growth was inhibited with no corresponding change in lung metastasis. In both models of AR activation, tumor collagen was not altered as measured by multiphoton SHG imaging or by standard immunostaining. In BALB/c mice with 4T1 tumors, ß2-AR elicited a tumor inhibitory environment that was not detected in C57BL/6 mice with EO771 tumors. In both mouse strains, unlike α2-AR activation, ß-AR activation alters myeloid populations, especially the immunosuppressive myeloid derived suppressor cells. A breast cancer cell line derived from the MMTV-PyMT mice was shown to possess functional alpha2-AR and ß-AR. We also show progress made in developing a model of micrometastasis after primary tumor dissection.

15. SUBJECT TERMS
Alpha2-adrenergic receptors, breast cancer, metastasis, dexmedetomidine, collagen, tumor associated fibroblasts, second harmonic generation

16. SECURITY CLASSIFICATION OF:			17. LIMITATION OF ABSTRACT	18. NUMBER OF PAGES	19a. NAME OF RESPONSIBLE PERSON
a. REPORT	b. ABSTRACT	c. THIS PAGE			19b. TELEPHONE NUMBER *(include area code)*
Unclassified	Unclassified	Unclassified	Unclassified	16	

Standard Form 298 (Rev. 8-98)
Prescribed by ANSI Std. Z39.18

Table of Contents

Page

1. INTRODUCTION

Despite advances in the treatment of breast cancer, metastatic disease remains a challenging clinical problem with few therapeutic options (1). Patients undergoing diagnosis and treatment of breast cancer often experience severe and chronic psychological stress. The sympathetic nervous system (SNS) is an important pathway by which psychological stress can promote tumor progression (reviewed in (2, 3)). The SNS neurotransmitters norepinephrine and epinephrine activate two major classes of adrenergic receptors (AR), α-AR (subdivided into α1 and α2) and ß-AR (subdivided into ß1, ß2, and ß3). The pro-tumor pathways activated by ß-AR stimulation have begun to be elucidated in breast and other cancers (4, 5), but there is a paucity of studies examining a role for α-AR activation, despite the fact that in human breast cancers, α-AR expression has been linked to poor prognosis (6). Only a few breast cancer cell lines have been demonstrated to express functional α-AR (7), but the host stromal cells that make up a tumor, including macrophages and fibroblasts, express α-AR and ß-AR normally (8-10) and in primary tumors (7). Here we describe progress made in defining the impact of α2-AR and ß-AR activation in C57BL/6 mice bearing EO771 mammary (orthotopic) tumors and in BALB/c mice with orthotopic 4T1 tumors. We also provide evidence that a breast cancer cell line derived from the MMTV-PyMT mice express both alpha2-AR and ß-AR. Finally, we show progress made in developing a model of micrometastasis after primary tumor dissection.

2. KEYWORDS

breast cancer, metastasis, alpha2-adrenergic receptors, ß-adrenergic receptors, dexmedetomidine, salmeterol, tumor associated fibroblasts, collagen, second harmonic generation, multiphoton laser scanning microscopy

3. ACCOMPLISHMENTS

What were the major goals of the project?

(The specific aims are the major goals of this project.)

Aim 1. Determine if α_2-AR-induced tumor progression and metastasis is a biological pathway common to many murine breast tumor models. *Progress reported below*.

Aim 2. Identify the cellular and molecular mechanism(s) underlying α_2-AR-induced tumor progression within 4T1 tumors. *Progress reported in YR1 Annual Report.*

Aim 3. Determine if DEX treatment during breast tumor surgery promotes micrometastasis. *Progress reported below.*

What was accomplished under these goals?

Describe 1) major activities; 2) specific objectives; 3) significant results or key outcomes, including major findings developments or conclusions (both positive and negative); and/or 4) other achievements.

SPECIFIC AIM 1

1) Major activities:

Specific aim 1: The effect of DEX treatment was determined in an orthotopic mammary tumor model, EO771 grown in syngeneic C57BL/6 mice. Salmeterol treatment to activate ß2-AR was tested in C57BL/6/EO771 and BALB/c/4T1 combinations. In addition, alpha2-AR and ß-AR expression was determined in a mammary tumor cell line (R221a) derived from the transgenic line, MMTV-PyMT, in which mice develop mammary tumors spontaneously.

Specific aim 3: Perfected the surgical technique for orthotopic tumor resection and made progress optimizing the frequency at which micrometastasis develop in distant organs.

2) Progress was made in each of the following specific objectives:

Specific aim 1a. Determined if α_2-AR activation by DEX increases tumor growth and metastases in the orthotopic mammary tumor model EO771 syngeneic with C57BL/6 mice.

1b. Determine if increased SHG-emitting collagen is a marker of α_2-AR-induced metastasis in tumor and in metastatic sites in C57BL/6 mice with orthotopic EO771.

1c. Identify tumor cytokines/chemokines altered by α_2-AR stimulation in orthotopic EO771 tumors.

1d. Determine if myeloid cells are modulated by α_2-AR stimulation in tumor and in distant sites by flow cytometry.

3) Significant results/key outcomes:

We have previously reported that DEX treatment increased 4T1 tumor growth and metastasis to the lung in BALB/c mice (11). In aim 1, we asked if the effect of alpha2-AR activation could be extended to other tumor models. The effect of DEX treatment on orthotopic EO771 mammary tumor growth and lung metastasis was assessed in C57BL/6 female mice. To elucidate the mechanisms underlying the effects of DEX, we tested for changes in the tumor extracellular matrix (collagen-emitting second harmonic generation (SHG)), cytokine/chemokine production by multianalyte analysis and immune cell populations by flow cytometric analyses.

We report here the following key findings:

Materials and Methods.

Drug Treatment. C57BL/6 female mice were injected intraperitoneally (IP) with sterile saline or 10 µg/kg DEX beginning 2 days prior to injection of $2x10^5$ tumor cells into a mammary fat pad and continuing daily through the day before sacrifice.

Tumor Growth. Tumor diameter was measured using calipers as described in (11).

SHG Imaging. The method for determining the F/B ratio of a thin tissue sample has been previously described (12). A Spectra Physics MaiTai Ti:Sapphire laser (power=0.1 mW for all imaging) was directed through an Olympus Fluoview FV300 scanner. This was focused through an Olympus water-immersion lens (20×, 0.95 NA), which subsequently captured backward propagating SHG signal. The SHG signal was separated from the excitation beam using a 670 nm dichroic mirror, filtered using a 405 nm filter, and collected by a photomultiplier tube. The forward scattered SHG was collected through an Olympus 0.9 NA condenser, reflected by a 565 nm dichroic mirror to remove excitation light, filtered by a 405 nm filter, and captured by a photomultiplier tube. Forward- and backward-scattered SHG images were simultaneously collected as a stack of 11 images spaced 3 µm apart with a 660-µm field of view. For each tissue section, 5 F/B images were collected (one in the center and 4 equi-distant points around the periphery of the section) and the average F/B ratio was calculated for each section. During acquisition of all SHG images, a dilute FITC fluorescein isothiocyanate solution was imaged to calibrate for day-to-day fluctuations in laser power.

Flow cytometry. Single cell suspensions were prepared from each tissue. Fc-receptor-mediated non-specific labeling was blocked by a 15-min incubation with anti-CD16/32. For myeloid cell populations, the following antibody panel was used: anti-CD45-blue violet; anti-CD11b-Alexafluor 647; anti-F4/80-FITC; anti-Gr-1-phycoerythrin. Color compensation was incorporated into all analyses. Negative controls were based on fluorescent minus one (FMO) background staining. For FMO autofluorescence, cells are incubated with all fluorophores except one, and the fluorescence intensity of the missing fluorophore was determined. The myeloid cell markers were gated based on CD45+ leukocytes. CD45 is a marker of all hematopoietic cells and is not expressed by tumor cells or fibroblasts.

Lung metastasis. Paraffin-embedded formalin-fixed lung tissue was sectioned into 5-micron sections. Three serial sections were mounted onto each slide and stained using hematoxylin and eosin (H&E). Five sets of serial sections were taken from each lung, 100 µm distance between each set. This spacing allows surveillance of metastatic lesions throughout the lung. A blinded observer determined the number of metastasis in each section using a brightfield microscope (4x magnification). The average number of lesions per three consecutive lung sections was calculated. This average was used to calculate the sum total of metastatic lesions in five sections per lung. Image analysis software was used to calculate the area of each metastatic lesion in each tissue section. The average lesion area was then determined for each mouse.

Statistical Analysis. Statistical analysis for all experiments was conducted with GraphPad PRISM software with $p<0.05$ considered statistically different. Outliers were determined using the Grubbs method and excluded from further analyses. In experiments with two experimental groups, an F-test for variance was conducted. If the variance was similar between groups ($p>0.05$), an unpaired, two-tailed student's t-test was employed. If the F-test for variance was significant ($p<0.05$), group comparisons were conducted using the non-parametric Mann-Whitney U-test.

A. Results: Dexmedetomidine (DEX) Treatment in female C57BL/6 mice

1. Tumor growth, metastasis, and SHG-emitting collagen (Objective 1a,b)

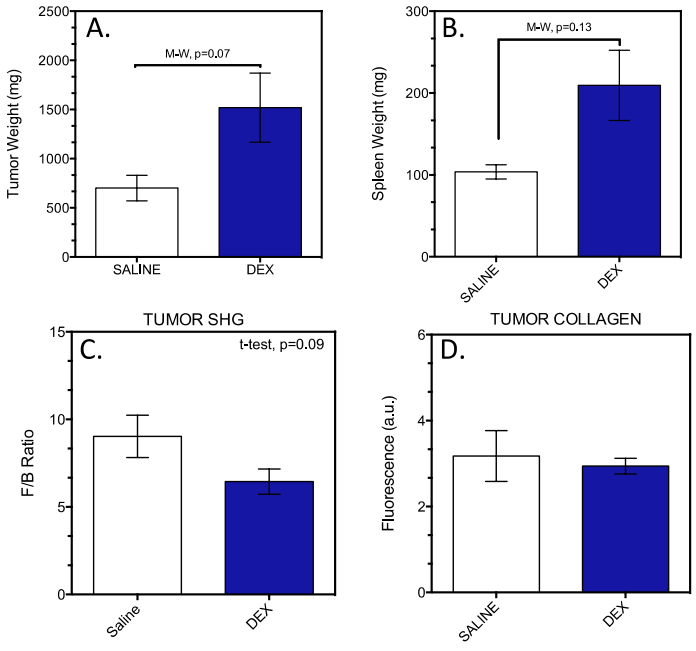

Fig. 1. Alpha2-AR activation promotes EO771 tumor progression and is associated with altered tumor SHG-emitting collagen. C57BL/6 females were treated daily with 10 µg/kg DEX or saline vehicle beginning 2 days before EO771 injection into a mammary fat pad. Mice were sacrificed 18 days after tumor cell injection. A,B. DEX increased tumor and spleen weight. C, D. Tumor SHG-emitting collagen was reduced with no change in total tumor collagen measured by immunohistochemical detection of type I fibrillar collagen. Results expressed as mean ± SEM. Saline, n=9, DEX, n=7. Statistical analysis determined by student's t-test or by non-parametric Mann-Whitney (M-W) U test.

In C57BL/6 mice, DEX treatment non-significantly ased tumor weight d 18 post-tumor cell injection 1A; p=0.07). In the EO771 model (like the 4T1 el), splenomegaly accompanies tumor growth and en weight is an indicator of tumor progression. A l to increased spleen weight was detected with DEX ment, consistent with elevated tumor weight (Fig. =0.13). In the tumors, a trend toward reduced SHG atio was detected (Fig. 1C; p=0.09) with no change tumor type-I collagen staining by standard unofluorescence (Fig. 1D). Lung metastatic lesions detected in all mice, but DEX did not significantly ge the number of lesions or lesion size (Fig. 2A,B; esentative images of lung metastasis in Fig. 2D-F). collagen SHG-emission (assessed as the forward sion to backward emission ratio (F/B ratio)) was not ed by DEX treatment (Fig. 2C). To determine if the l toward increased tumor progression with alpha2-activation was associated with infiltration of pro- r myeloid populations, flow cytometric analysis of 5+ pan leukocyte populations was conducted using markers CD11b, Gr-1, and F4/80 to distinguish 1b+Gr-1+ myeloid derived suppressor cells SC), CD11b+Gr-1- monocytes, and CD11b+F4/80+ r associated macrophages (TAMs). In the tumors, y immunosuppressive MDSC were reduced with DEX treatment (Fig. 3), but no significant alterations were detected in MDSC frequency in spleen (p=0.22) and metastatic lung (p=0.17) (Fig. 3). DEX-induced alterations in the other myeloid populations were not detected (Fig. 3). These results indicate a reduction in the frequency in MDSC populations in the tumor with alpha2-AR activation that is not consistent with increased tumor growth.

To assess the cytokine/chemokine milieu within the tumors, a multiplex analysis was conducted. Trends in several cytokines were apparent, with significant reductions in anti-inflammatory IL-10 (t-test, p=0.002) and VEGF (p=0.04) (Fig. 4). DEX treatment did not alter tumor MMP-2, -3, and -9 (Fig. 4). The reduction in MDSC frequency is consistent with a reduction in IL-10 and VEGF (13), but they do not explain DEX-induced increase in tumor weight. On the other hand, the trend toward reduced IL-12, IFN-γ and elevated G-CSF and MIP-2 give clues that other cell populations and/or effector functions that promote tumor growth may be altered by DEX treatment. For example, IFN-γ is associated with effector function of natural killer cells and CD8+ tumor cells, both sources of effective anti-tumor immunity. G-CSF and MIP-2 are associated with tumor progression. Together these non-significant changes indicate other mechanisms that contribute to the elevated tumor growth observed with DEX treatment.

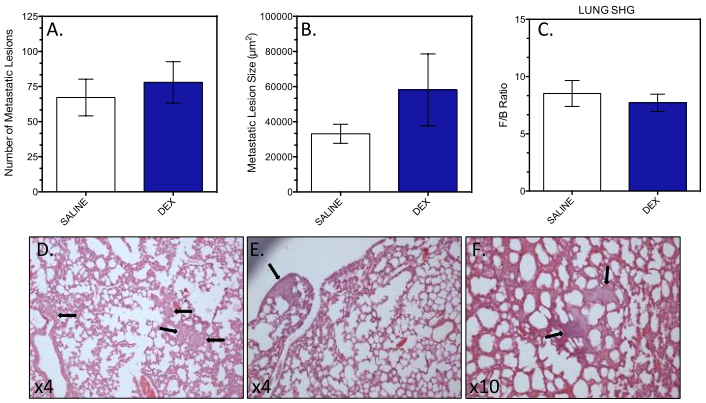

Fig. 2. Lung metastatic lesions were not significantly altered by alpha2-AR activation. Lung metastases were determined by quantifying metastatic lesions in 5 tissue sections distributed equally across the entire lung. A. Number of metastatic lesions B. Lesion size determined by image analysis software. (M-W, p=0.34). C. Lung SHG-emitting collagen determined in regions of interest adjacent to metastatic lesions. D-F are representative H&E stained images. Results expressed as mean ± SEM. Saline, n=9, DEX, n=7.

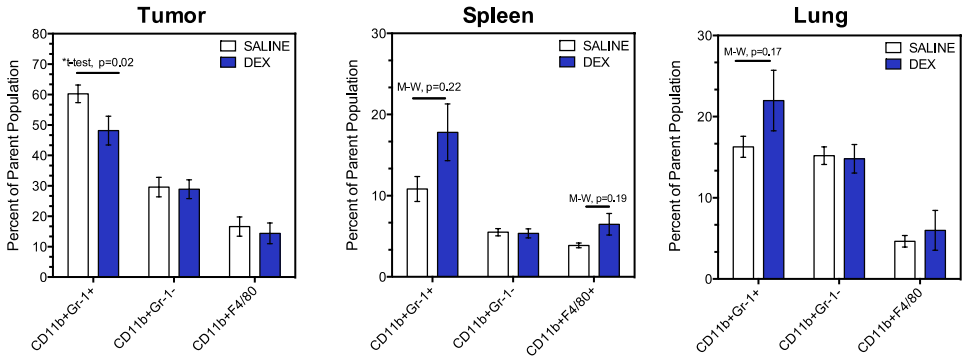

Fig. 3. Alpha2-AR activation and myeloid populations in tumor, spleen, and lung of EO771-bearing mice. In tumors, DEX decreased tumor CD11b+Gr-1+ MDSC, but not other other myeloid populations. In spleen and lung, DEX did not significantly alter any myeloid populations. Results expressed as mean ± SEM. Saline, n=9, DEX, n=7. Statistical analysis determined by student's t-test or by non-parametric Mann-Whitney (M-W) U test.

CUSSION. These results onstrate trends in EO771 tumor ression associated with DEX ment as we reported previously ne 4T1/BALB/c tumor model. ever, the effects are not as inent as in BALB/c mice. The ations are not clearly ciated with alterations in SC and may be dependent on ctions in anti-tumor cell unity.

er Significant ults/Achievements: The endogenous ligands for □□□□□2-AR are the catecholamines norepinephrine and epinephrine. These catecholamines have mixed affinity for α-AR and ß-AR. Thus the AR activated is dependent on the local concentration of norepinephrine. In the previous annual report, we demonstrated opposite effects of DEX (□□□□□2-AR agonist) compared to salmeterol (ß2-AR agonist) on 4T1 tumor growth and metastasis. This raises questions regarding the impact of NE released under stress (high local concentration) versus non-stress (low local concentration) conditions. ß-AR activation has been shown to promote tumor progression in tumor models in which the tumor cells express functional ß-AR (4, 5). In the BALBc/4T1 mammary tumor model, we observed unexpected tumor inhibitory effects including reduced metastatic lesions with the highly selective ß2-AR agonist salmeterol (SALM). To determine if the inhibitory effects of ß2-AR activation are limited to the 4T1 model, the impact of SALM treatment in the C57BL/6/EO771 mammary tumor model was tested.

Materials and Methods.

Drug Treatment. Mice were injected intraperitoneally (IP) with sterile saline or 5 mg/kg salmeterol beginning 2 days prior to injection of $2x10^5$ tumor cells into a mammary fat pad and continuing daily through the day before sacrifice.

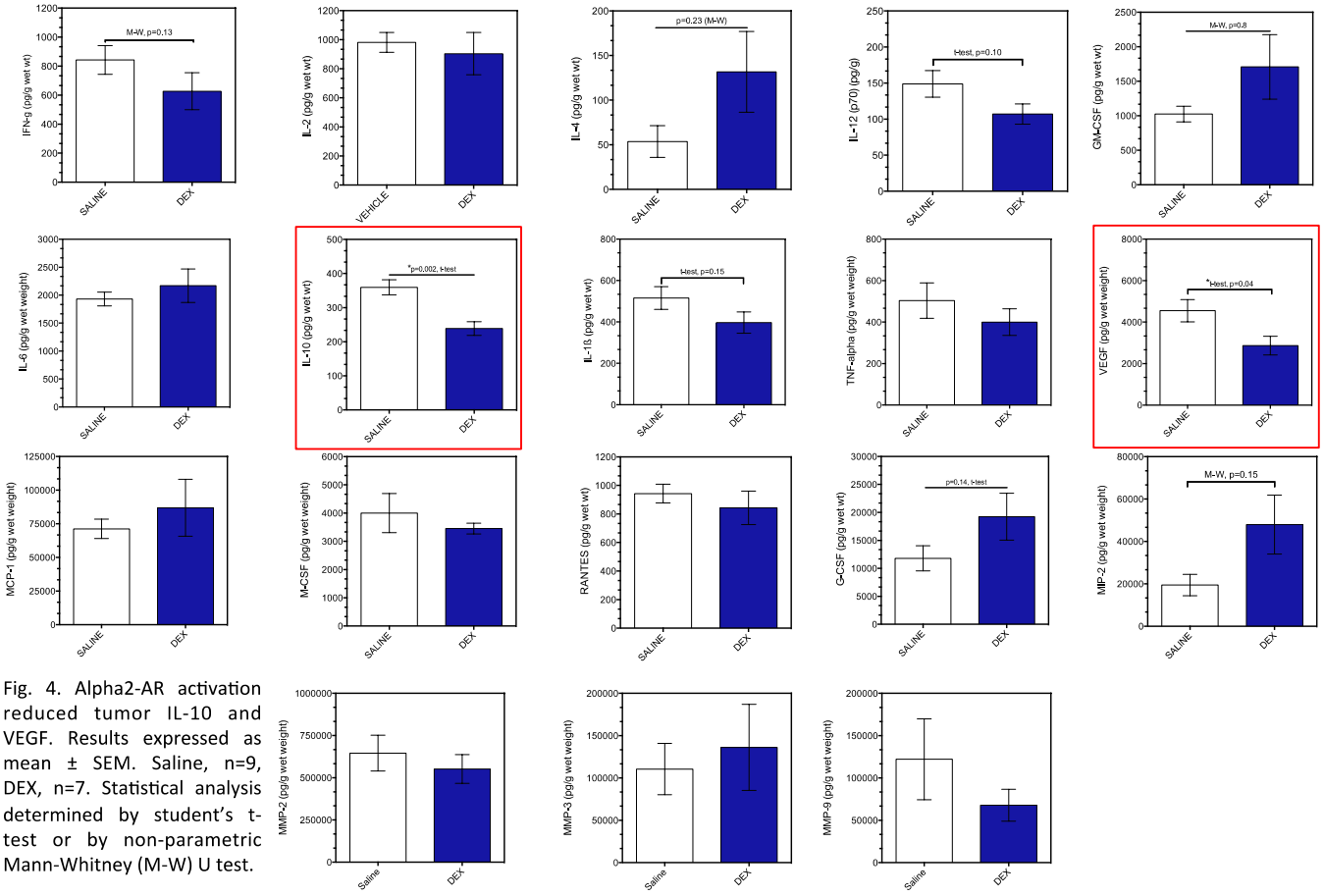

Fig. 4. Alpha2-AR activation reduced tumor IL-10 and VEGF. Results expressed as mean ± SEM. Saline, n=9, DEX, n=7. Statistical analysis determined by student's t-test or by non-parametric Mann-Whitney (M-W) U test.

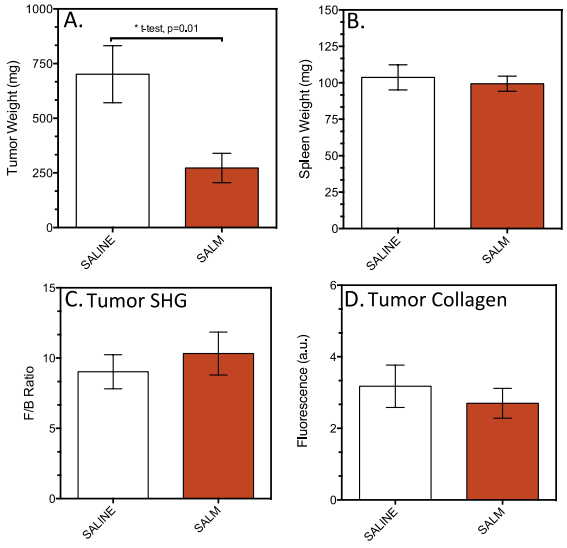

Fig. 5. ß2-AR activation reduced EO771 tumor weight. C57BL/6 females were treated daily with 5 mg/kg salmeterol (SALM) or saline vehicle beginning 2 days before EO771 injection into a mammary fat pad. Mice were sacrificed 18 days after tumor cell injection. A, B. SALM decreased tumor but not spleen weight. C,D. SALM did not alter tumor SHG total tumor collagen as measured by immunohistochemical detection of type I fibrillar collagen. Results expressed as mean ± SEM. Saline, n=9, SALM, n=9.

All other methods as described above.

B. Results: Salmeterol (SALM) Treatment in Female C57BL/6 mice

2. Tumor growth, metastasis, and SHG-emitting collagen (Objective 1a,b)

In C57BL/6 mice, SALM significantly reduced tumor weight 18 days after EO771 injection (p=0.01; Fig. 5). Spleen weight was not reduced (Fig. 5B), but the lack of an effect is most likely a 'floor effect' because spleen weight in healthy, non-tumor bearing C57BL/6 mice averages ~100 mg indicating that splenomegaly had not yet occurred at this time point. SALM did not alter tumor SHG-emitting collagen (Fig. 5C) or collagen type I immunostaining (Fig. 5D). Lung metastatic lesion number and size and lung SHG F/B ratio were not significantly altered by SALM treatment (Fig. 6).

The SALM-induced reduction in tumor weight was associated with reduced frequency of tumor MDSC (p=0.017) and a trend towards reduced MDSC in spleen (p=0.059) (Fig. 7). SALM did not alter lung MDSC frequency (Fig. 7). On the other hand, SALM increased CD11b+Gr-1- monocytes and CD11b+F4/80+

macrophages in the metastatic lung, with similar trends in the spleen, but not in tumors (Fig. 7). SALM-induced reduction in tumor growth was associated with few changes in tumor cytokines and chemokines except a significant decrease in RANTES, a recruiter of tumor MDSC (14) (Fig. 8).

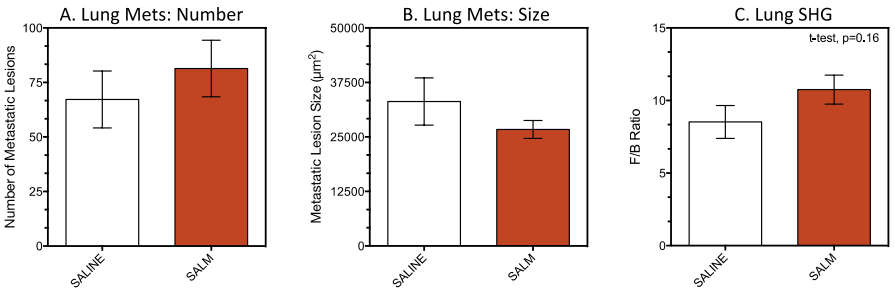

Fig. 6. EO771 lung metastatic lesions were not significantly altered by ß2-AR activation. A. Number of metastatic lesions. B. Lesion size determined by image analysis software (M-W, p=0.8). C. Lung SHG-emitting collagen determined in regions of interest adjacent to metastatic lesions. Results expressed as mean ± SEM. Saline, n=9, SALM, n=9.

Discussion. SALM treatment in the C57BL/6-EO771 model reduced tumor growth in association with reduced tumor MDSC. These results are similar to the tumor inhibitory environment observed in SALM-treated BALB/c-4T1 model (see results below and Annual Report Year 1). However, the EO771 model did not show any change in lung metastasis and demonstrated no association with tumor SHG, unlike 4T1. These results imply that the impact of ß2-AR activation on MDSC is independent of mouse strain/tumor, but the metastatic outcome may be dependent on tumor and/or genetic background. Tumor progression in mouse metastatic models breast cancer, as in human breast cancer, elicits mobilization of MDSC from the bone marrow to spleen and tumor, and these processes that have been shown to be regulated in normal mice by norepinephrine (15, 16). The reduction in tumor

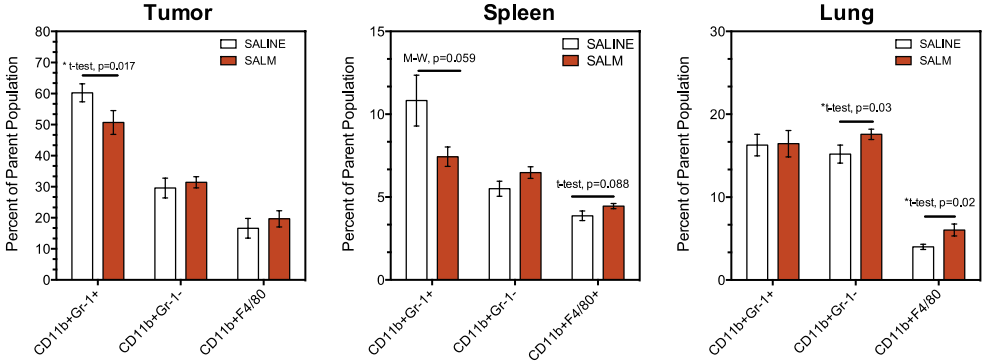

Fig. 7. ß2-AR activation and myeloid populations in tumor, spleen, and lung of EO771-bearing mice. SALM decreased tumor and spleen CD11b+Gr-1+ MDSC. In spleen and lung, SALM increased CD11b+F480+ macrophages and CD11b+Gr-1- monocytes. Results expressed as mean ± SEM. Saline, n=9, DEX, n=9. Statistical analysis determined by student's t-test or by non-parametric Mann-Whitney (M-W) U test.

TES may reduce the number DSC entering the tumor (14). natively, ß2-AR activation may MDSC differentiation toward re CD11b+ Gr-1- monocytes CD11b+ F4/80+ tumor ciated macrophages (17). ence for this latter mechanism ost apparent in the spleen e reduced frequency of MDSC accompanied by increased ency in the mature 1b+Gr-1- and CD11b+F4/80+ lations.

Overall, these results demonstrate distinct patterns in a tumor's response to alpha2 versus ß-AR activation, and that these effects are independent of tumor model and mouse strain. This implies that norepinephrine produces distinct and often opposite effects on tumor progression, depending on the local concentration of norepinephrine. In preliminary results, we have evidence that EO771 are similar to 4T1 in being unable to respond to ß-AR signaling as measured by cell surface ß-AR expression. Therefore these effects may be indicative of host stromal cell AR expression and function in the absence of direct activation of tumor cell AR.

These experimental results are also significant because they reveal tumor inhibitory effects of ß-AR activation that go against the prevailing view that ß-AR activation accelerates breast cancer progression (4, 5). Therefore, to further explore ßAR-induced tumor inhibition, we assessed the kinetics of the SALM-induced alterations in tumor progression in the BALB/c-4T1 model.

To clarify if SALM elicited a long term versus a transient tumor inhibitory microenvironment, 4T1 tumor-bearing mice treated with vehicle or SALM and sacrificed at 2 different time points in tumor progression. In this experiment, SALM treatment did not alter tumor weight at 14 or 21 days (Fig. 9A). Nonetheless, systemic inhibitory effects were observed with SALM treatment, including a significant reduction in spleen weight at d 21 (Fig. 9B). Spleen weight correlates with tumor progression in 4T1 tumor-bearing mice (11).

SALM also decreased lung metastatic lesions at d14 post- 4T1 injection (Fig. 9C), but not size (Fig. 9D).

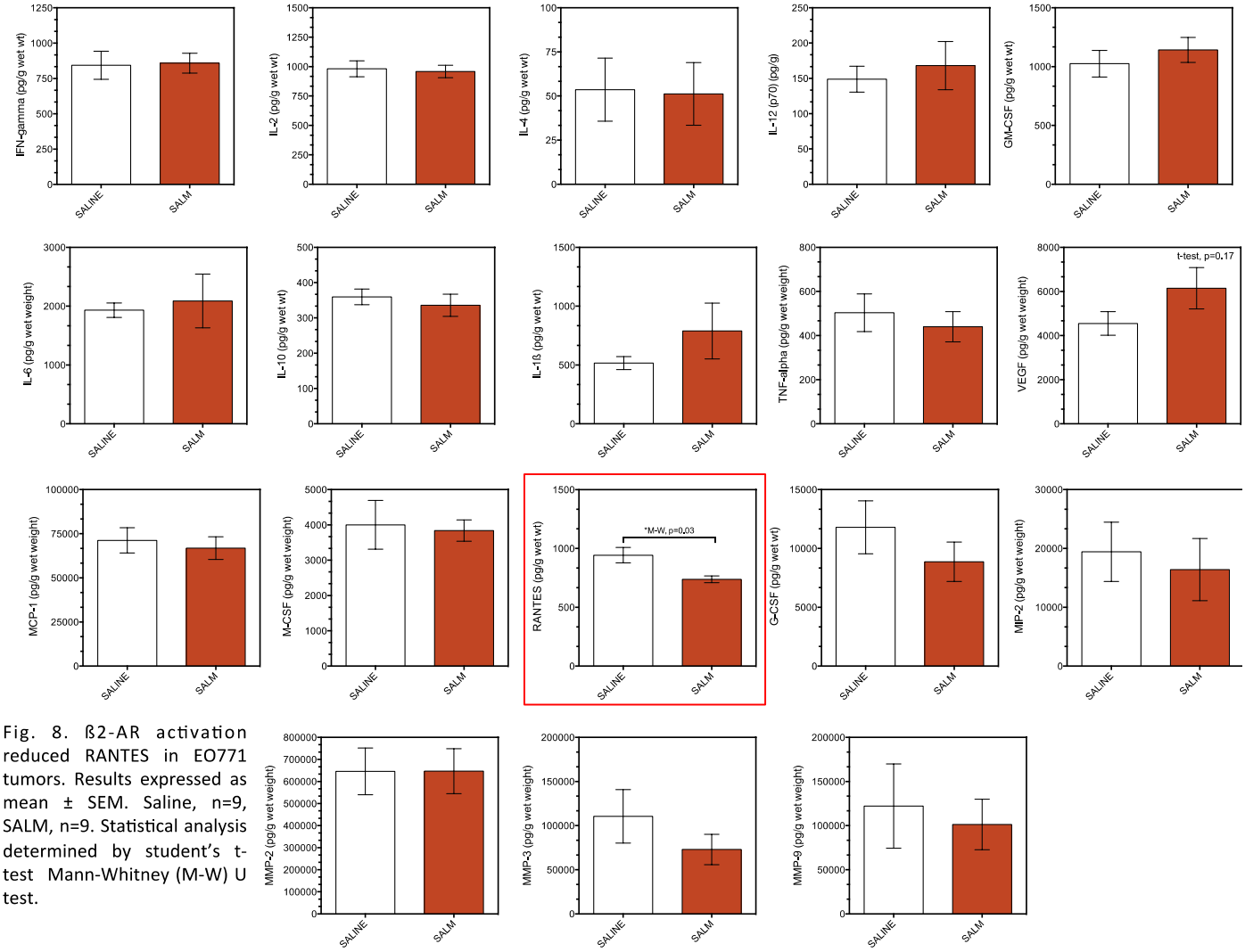

Fig. 8. ß2-AR activation reduced RANTES in EO771 tumors. Results expressed as mean ± SEM. Saline, n=9, SALM, n=9. Statistical analysis determined by student's t-test Mann-Whitney (M-W) U test.

Furthermore, in a time-dependent fashion, SALM treatment reduced tumor production of the pro-inflammatory cytokine IL-10 (Fig. 10A), IL-6 (Fig. 10B), G-CSF (Fig. 10C), and the recruiters of myeloid populations MCP-1 (CCL-2) (Fig. 10D) and MIP-2 (Fig. 10E). Flow cytometric analysis of myeloid populations in the tumor revealed no SALM-induced changes, but in the spleen and lung the frequency of CD11b+Gr-1+ MDSC was elevated at d 14 and reduced by day 21 with SALM treatment (Fig. 11A). The frequency of F4/80+ TAMs was not altered in tumor, spleen, or lung at either time point (Fig. 11B). However, SALM reduced CD8+, CD4+, and CD4+CD25+ Treg frequency in the tumor at d 14 (Fig. 12).

DISCUSSION. Together these data suggest that ß-AR activation induced an inhibitory microenvironment within the tumor and was associated with early, but transient inhibition of lung metastasis. The early SALM-induced reduction in the tumor chemokines MCP-1 and MIP-2 would be predicted to reduce tumor myeloid population frequency, but the tumor myeloid populations were not altered at either time point. However, MDSC were elevated in spleen and lung at d14 and inhibited at

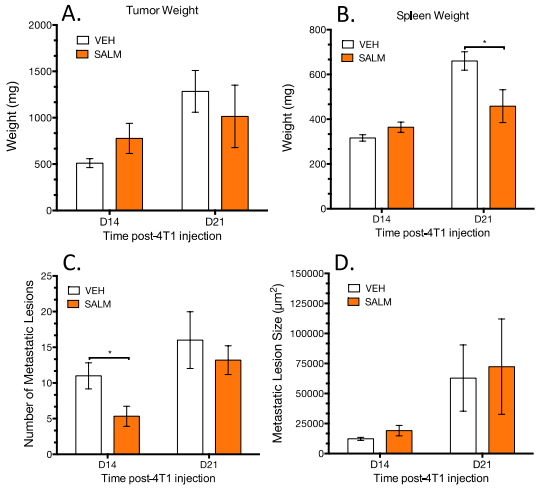

Fig. 9. Kinetics of the response to ß2-AR activation in the 4T1 orthotopic tumor model. BALB/c females were treated daily with 5 mg/kg salmeterol (SALM) or saline vehicle beginning 2 days before 4T1 injection into a mammary fat pad. Mice were sacrificed 14 or 21 days after tumor cell injection. A, B. SALM did not alter tumor weight but reduced spleen weight late in tumor progression. C,D. SALM reduced the number of lung metastatic lesions, but not metastatic lesion size. Results expressed as mean ± SEM. Saline, n=9, SALM, n=9; *P<0.05.

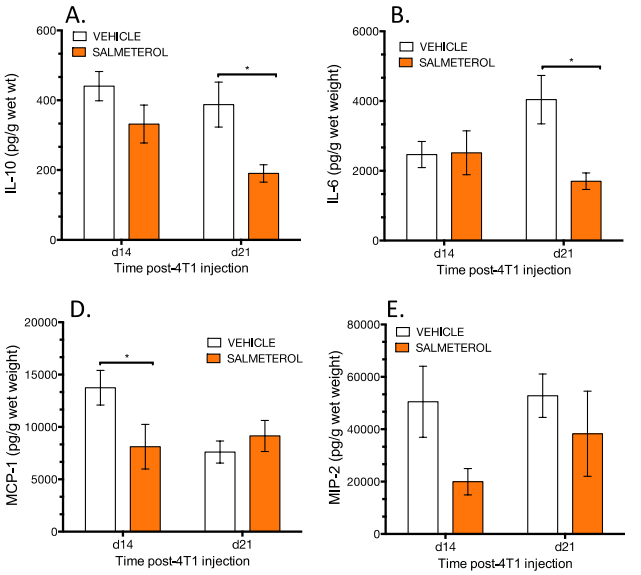

Fig. 10. SALM-induced reduction in 4T1 tumor cytokines. BALB/c female mice were treated daily with 5 mg/kg SALM or saline vehicle beginning 2 days before 4T1 injection into a mammary fat pad. Mice were sacrificed 14 or 21 days after tumor cell injection. Results expressed as mean ± SEM. Saline, n=9, SALM, n=9; *p<0.05.

d21 suggesting that the MDSC retained in spleen and/or erentially migrated to the lung. reduction in the tumor pro- mmatory cytokines would also ict reduced lung metastatic ns, especially decreased G- (18), however, there was only ransient reduction in lung static lesion size. This ests that other mechanisms active to counter-act SALM- ced tumor inhibitory effects. M treatment reduced the CD8+ lation at d14, consistent with work of Repalsky and agues (19), and suggests that tumor immunity mediated by CD8+ cytotoxic T lymphocytes was impeded with SALM treatment. This also may be a mechanism that counters the reduced pro-tumor cytokines. As we have observed previously, MDSC were sensitive to ß-AR activation, and as pointed out in discussion above, may have mediated by alterations in C migratory behavior. ever, in this experiment, SALM not appear to modify tumor ation by MDSC. The frequency 1/80+ TAMs does not appear to ensitive to ß-AR activation in tumor, spleen, or lungs. This against the observation that R activation in vivo increased r metastasis by recruiting 1b+F4/80+ TAMs (5). We thesize that the difference een these two tumor models cts ß-AR activation status of tumor cells. Sloan and agues (5) demonstrated that orthotopic tumor model, a nt of the 4T1 tumor model in B/c mice, expressed functional R, while we have demonstrated that 4T1 does not express functional ß-AR (11). Furthermore, the SALM-induced increase in lung CD11b+Gr-1+ MDSC is not consistent with the reduced metastasis seen early in the response. Together these results suggest that ß-AR activation of multiple tumor populations (tumor cells and host stromal cell populations) contributes to differences in the response to ß-AR activation in tumor progression. Finally, ß-AR desensitization may elicit the transiency of the response, although we have tried to minimize the impact of desensitization by using the long-acting SALM.

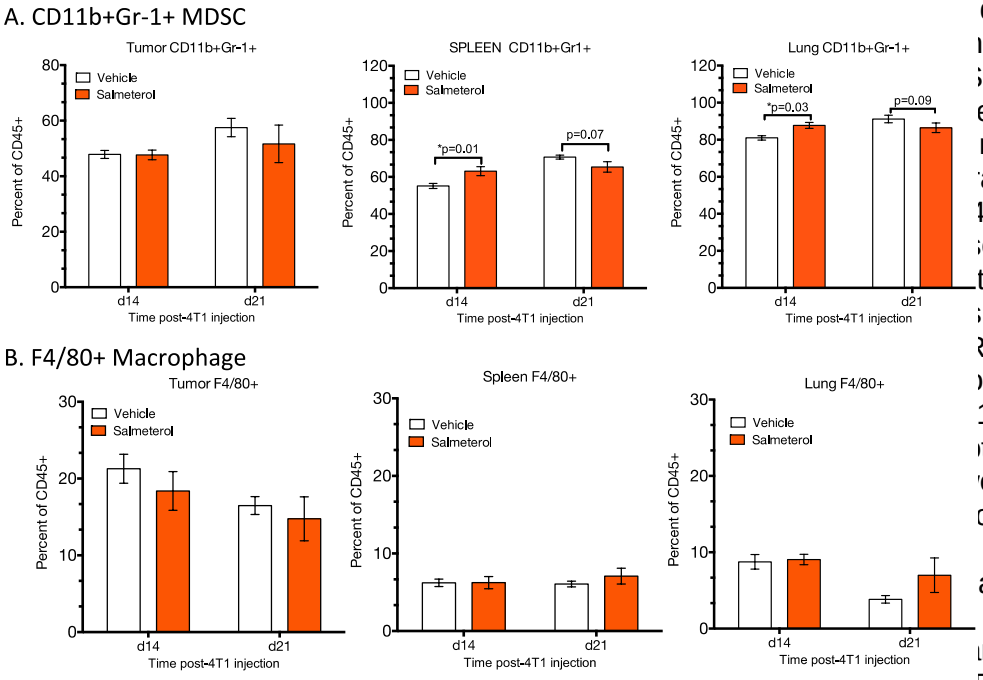

Fig. 11. SALM-induced reduction in 4T1 MDSC and macrophages. BALB/c female mice were treated daily with 5 mg/kg SALM or saline vehicle beginning 2 days before 4T1 injection into a mammary fat pad. Mice were sacrificed 14 or 21 days after tumor cell injection. Results expressed as mean ± SEM. Saline, n=9, SALM, n=9; *P<0.05.

C. AR Expression in Tumor Cells from MMTV-PyMT mice.

In our previous work (11), we demonstrated that alpha2-AR activation promoted tumor progression in the 4T1 orthotopic model, despite the fact that 4T1 tumor cells do not express alpha2-AR. As discussed above, we hypothesize that differences in AR responses between tumor models are partially related to AR expression levels of the tumor . In the YR1 annual report, had tested the response to in MMTV-PyMT mice. To acterize AR signaling city in tumor cells derived MMTV-PyMT mammary rs, intracellular cAMP was sured in response to ctive agonists. Upon ligand ng, alpha2-AR couple to Gi eins to inhibit adenylate ase and thereby reduce P. We demonstrate here that cell line R221a, derived from MMTV-PyMT mice, expresses functional alpha2-AR as demonstrated by the finding that 2 selective alpha2-AR agonists, DEX and clonidine reduced forskolin-induced cAMP (Fig. 13A). ß-AR activate adenylate cyclase through Gs to elevate intracellular cAMP. R221a cells express functional R as demonstrated by the ability of the selective ß-agonist isoproterenol and ß2-AR-selective agonist formoterol to ase cAMP (Fig. 13B). However, the induced response was much greater was produced at a lower concentration ive to formoterol. To explain the rential in the cAMP response to these l agonists, we are currently testing if La cells express ß1- or ß3-AR, in ion to ß2-AR. ß1 and ß3-AR are ated by isoproterenol, unlike oterol.

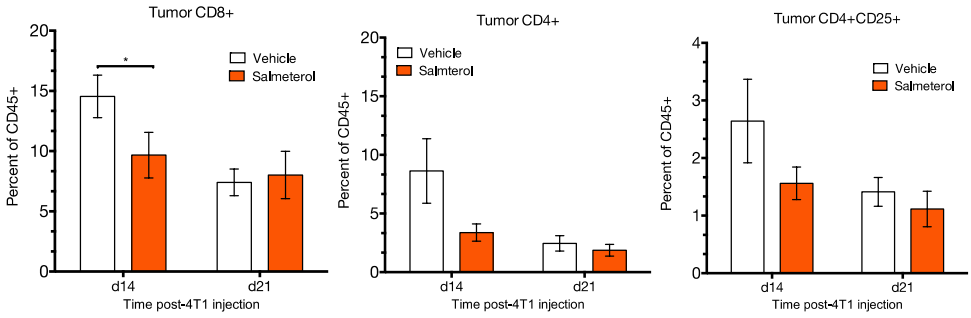

Fig. 12. SALM-induced reduction in 4T1 T cell subpopulations. BALB/c female mice were treated daily with 5 mg/kg SALM or saline vehicle beginning 2 days before 4T1 injection into a mammary fat pad. Mice were sacrificed 14 or 21 days after tumor cell injection. Results expressed as mean ± SEM. Saline, n=9, SALM, n=9; *p<0.05.

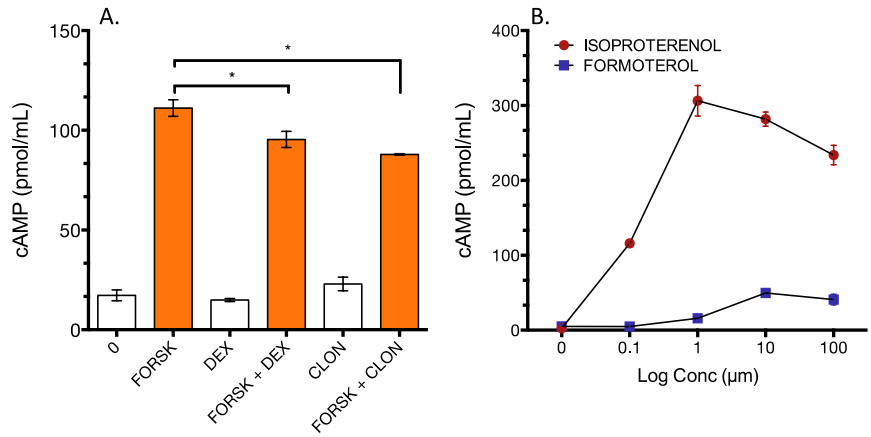

Fig. 13. R221a, a cell line derived from MMTV-PyMT tumors, express (A) α_2-AR and (B) ß2-AR based on signaling capacity. cAMP-induced forskolin (FORSK, 50 µm) is reduced by 2 α_2-AR-selective agonists dexmedetomidine (DEX, 0.1 µM) and clonidine (CLON, 0.1 µM). (B) Isoproterenol (non-selective ß-AR) and formoterol (ß2-AR selective) elevated intracellular cAMP in R221a cells. *p<0.05.

CIFIC AIM 3

ajor activities: Determine if DEX ment during breast tumor surgery promotes micrometastasis.

Methods. *IVIS Imaging.* In BALB/c mice, luc2-transfected-4T1 cells (Caliper Life Sciences) were employed to image tumor growth *in vivo*. For IVIS imaging, mice were injected IP with luciferin (Caliper; 150 mg/kg) in sterile saline. Five minutes later, mice were anesthetized using 90 mg/kg ketamine plus 10 mg/kg xylazine. Mice were placed in the heated (37˚C) imaging chamber. Images were taken every 30 secs for 5 minutes.The goal of these experiments is to determine if acute α_2-AR activation in the surgical setting will impact the development of micrometastasis associated with breast tumor resection.

The first objective has been to establish that surgical resection of 4T1 tumors establishes lung micrometastasis in our hands. With the assistance of the University of Rochester vivarium staff, we can now surgically resect the tumors very cleanly with no detectable residual tumor tissue based on IVIS imaging using d-luciferase-transfected 4T1 tumor cells (Fig. 14). We have tested surgery at 2 time points after tumor cell injection (Day 4 and Day 7), and imaged mice weekly to determine if distant site metastases were detectable. Thus far, we have detected distant metastasis in 1 mouse (out of 4 tested) 15 days after surgical resection (Fig. 14). The tumors in this group of mice were removed 7 days after tumor cell injection. We continue to follow this group of mice and the other mice in which tumors were

removed 4 days after tumor cell injection. We will continue to identify the timing in which a larger proportion of mice that have undergone surgery will develop distant metastases. All mice will be continually followed and eventually sacrificed. At sacrifice, distant secondary tissues (lung, spleen, and bone marrow) will be fixed and H&E stained to determine if metastatic lesions are present and compared to IVIS imaging detection.

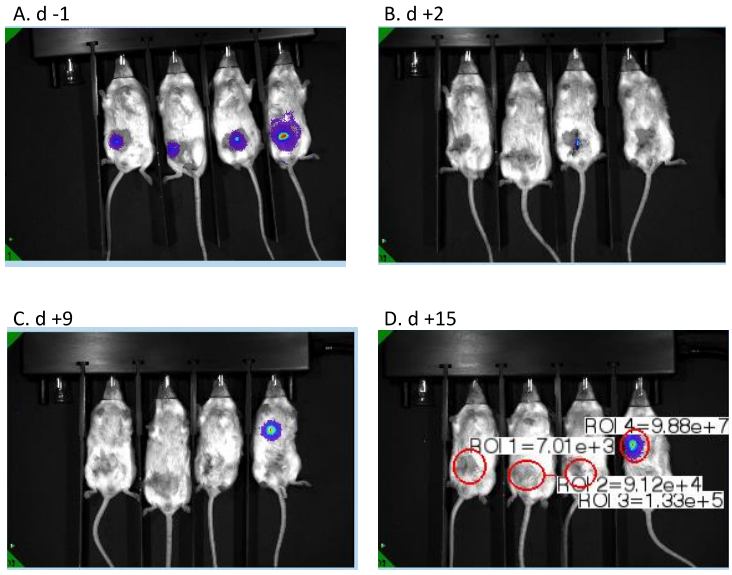

Fig. 14. IVIS imaging of dluc-4T1 tumor before and after primary tumor resection in the same 4 mice. IVIS imaging was conducted prior to (A) and 2 d (B) after surgery to confirm the clean removal of 4T1 tumor cells. By 9 days after surgery, 1 mouse had developed a distant metastasis in the region of the lung. The values in D represent total flux in photon/sec determined in the region of interest. Multiple exposure times were tested. This series of images represents 30 sec exposure.

REFERENCES CITED

1. Steeg PS. Tumor metastasis: mechanistic insights and clinical challenges. Nat Med. 2006;12:895-904.
2. Antoni MH, Lutgendorf SK, Cole SW, Dhabhar FS, Sephton SE, McDonald PG, et al. The influence of bio-behavioural factors on tumour biology: pathways and mechanisms. Nat Rev Cancer. 2006;6:240-8.
3. Cole SW, Nagaraja AS, Lutgendorf SK, Green PA, Sood AK. Sympathetic nervous system regulation of the tumour microenvironment. Nat Rev Cancer. 2015;15:563-72.
4. Thaker PH, Han LY, Kamat AA, Arevalo JM, Takahashi R, Lu C, et al. Chronic stress promotes tumor growth and angiogenesis in a mouse model of ovarian carcinoma. Nat Med. 2006;12:939-44.
5. Sloan EK, Priceman SJ, Cox BF, Yu S, Pimentel MA, Tangkanangnukul V, et al. The sympathetic nervous system induces a metastatic switch in primary breast cancer. Cancer Res. 2010;70:7042-52.
6. Powe DG, Voss MJ, Habashy HO, Zanker KS, Green AR, Ellis IO, et al. Alpha- and beta-adrenergic receptor (AR) protein expression is associated with poor clinical outcome in breast cancer: an immunohistochemical study. Breast Cancer Res Treat. 2011;130:457-63.
7. Bruzzone A, Pinero CP, Rojas P, Romanato M, Gass H, Lanari C, et al. alpha(2)-Adrenoceptors enhance cell proliferation and mammary tumor growth acting through both the stroma and the tumor cells. Curr Cancer Drug Targets. 2011;11:763-74.
8. Wang Q, Lu R, Zhao J, Limbird LE. Arrestin serves as a molecular switch, linking endogenous alpha2-adrenergic receptor to SRC-dependent, but not SRC-independent, ERK activation. J Biol Chem. 2006;281:25948-55.

9. Spengler RN, Allen RM, Remick DG, Strieter RM, Kunkel SL. Stimulation of alpha-adrenergic receptor augments the production of macrophage-derived tumor necrosis factor. Journal of Immunology. 1990;145:1430-4.
10. Nance DM, Sanders VM. Autonomic innervation and regulation of the immune system (1987-2007). Brain Behav Immun. 2007;21:736-45.
11. Szpunar MJ, Burke KA, Dawes RP, Brown EB, Madden KS. The Antidepressant Desipramine and alpha2-Adrenergic Receptor Activation Promote Breast Tumor Progression in Association with Altered Collagen Structure. Cancer Prev Res (Phila). 2013;6:1262-72.
12. Burke K, Tang P, Brown E. Second harmonic generation reveals matrix alterations during breast tumor progression. J Biomed Opt. 2013;18:31106.
13. Markowitz J, Wesolowski R, Papenfuss T, Brooks TR, Carson WE, 3rd. Myeloid-derived suppressor cells in breast cancer. Breast Cancer Res Treat. 2013;140:13-21.
14. Zhang Y, Lv D, Kim HJ, Kurt RA, Bu W, Li Y, et al. A novel role of hematopoietic CCL5 in promoting triple-negative mammary tumor progression by regulating generation of myeloid-derived suppressor cells. Cell Res. 2013;23:394-408.
15. Scheiermann C, Kunisaki Y, Lucas D, Chow A, Jang JE, Zhang D, et al. Adrenergic nerves govern circadian leukocyte recruitment to tissues. Immunity. 2012;37:290-301.
16. Jin J, Wang X, Wang Q, Guo X, Cao J, Zhang X, et al. Chronic psychological stress induces the accumulation of myeloid-derived suppressor cells in mice. PLoS One. 2013;8:e74497.
17. Yan HH, Pickup M, Pang Y, Gorska AE, Li Z, Chytil A, et al. Gr-1+CD11b+ myeloid cells tip the balance of immune protection to tumor promotion in the premetastatic lung. Cancer Res. 2010;70:6139-49.
18. Cao Y, Slaney CY, Bidwell BN, Parker BS, Johnstone CN, Rautela J, et al. BMP4 inhibits breast cancer metastasis by blocking myeloid-derived suppressor cell activity. Cancer Res. 2014;74:5091-102.
19. Eng JW, Reed CB, Kokolus KM, Pitoniak R, Utley A, Bucsek MJ, et al. Housing temperature-induced stress drives therapeutic resistance in murine tumour models through beta2-adrenergic receptor activation. Nat Commun. 2015;6:6426.
20. Cole SW, Sood AK. Molecular pathways: beta-adrenergic signaling in cancer. Clin Cancer Res. 2012;18:1201-6.

4. IMPACT

What was the impact on the development of the preliminary discipline of the project? The results indicate that the tumor promoting effect of alpha2-AR activation is observable in the C57BL/7 mouse-EO771 combination but the underlying mechanisms appear to differ from that of BALB/c-4T1. The results confirm that changes in tumor SHG F/B ratio is associated with altered metastasis to the lung, and may be useful an indicator of future metastatic effects. An important finding is that the effect of ß2-AR activation is opposite to that of alpha2-AR activation. This result has implications with regard to the effect of the endogenous ligand norepinephrine. Norepinephrine may elicit different tumor responses depending on its local concentration; higher concentrations, such as those obtained following stress-induced release of norepinephrine will activate ß2-AR and alpha2-AR; baseline levels of norepinephrine may only activate surrounding target cells that express alpha2-AR. In the 4T1 and EO771 tumor models used here, the tumor cells do not express functional ß-AR. Here we demonstrate functional alpha2-AR and ß-AR in tumor cells derived from the MMTV-PyMT model. This will be important as we determine the impact of sympathetic nervous system activation in MMTV-PyMT mice, a model that closely mimics human hormone receptor-expressing cancers. We contend that the impact of AR activation on host AR-expressing stromal cells needs to be distinguished from that of AR-expressing tumor cells. Our results point to the potential for stress exposure and sympathetic nervous system activation to have bi-directional effects on cancer

progression. In the context of personalized medicine, AR expression may be important in predicting an individuals' cancer response to stressor exposure.

The finding that ß2-AR activation inhibits pathways, including reduced G-CSF, IL-6 and CCL2 (MCP-1) that promote tumor progression has clinical implications. ß-AR blockers have been proposed as a new therapy in the treatment of breast cancer (20). These results suggest that caution should be used in the clinical use of ß-blockers until it can be clarified when ß-blockade will be safe and effective.

What was impact on other disciplines, technology transfer, and on society beyond science and technology? Nothing to report.

5. CHANGES/PROBLEMS:

Our ability to conduct the experiments proposed for specific Aim 3 is problematic because of the low rate of development of metastasis in distant organs in the 4T1 model. We have observed lung metastasis in 1 out of 20 mice who have undergone successful surgery (i.e. no detectable primary tumor). We will continue to observe and image these mice to determine if distant metastasis will eventually develop, but we are concerned that our ability to determine the impact of DEX treatment around the time of surgery will be compromised with such a low level of metastasis detected. It is possible that the length of time required to develop micrometastasis may be sufficient for the 4T1-dluc cells to lose the luciferase transgene required for IVIS imaging. For now, any mice that develop metastasis to distant sites as detected with IVIS imaging or become ill (even without detectable metastasis by IVIS imaging) will be sacrificed for ex vivo imaging of lung, bone marrow, spleen to determine if signal is detectable in any of these potential metastatic sites. In addition, we will histologically assess micrometastatic lesions detections using standard H&E staining with assistance from Dr. Ping Tang, surgical pathologist. This will help us determine if under our conditions, the development of micrometastasis is a rare event and a new approach will be needed to assess the development in orthotopic models.

6. PRODUCTS:

Publications, conference papers, and presentations:

PRESENTATIONS

Madden, K.S., Dawes, R.P., D.K. Byun, E.B. Brown. 2014. $ß_2$-Adrenergic Agonist Treatment Inhibits 4T1 Breast Tumor Metastasis to the Lung. Annual Psychoneuroimmunology Research Society Scientific Meeting, Philadelphia, PA. (Oral Presentation)

Roswell Park Cancer Institute (RPCI), Buffalo, NY. April 28, 2015. "Psychosocial Stress Exposure and Sympathetic Nervous System Activation in Preclinical Models of Breast Cancer" Invited by Dr. Elizabeth Repasky, Professor of Immunology, RPCI.

University of Rochester Medical Center; Current Issues in Breast Cancer. "Psychosocial Stressors and Sympathetic Nervous System Activation in Preclinical Models of Breast Cancer" November 11, 2015.

University of Rochester Medical Center; Department of Pathology and Laboratory Medine. "Sympathetic Nervous System and Adrenergic Receptor Activation in Preclinical Models of Breast Cancer" January 18, 2016.

POSTERS

Dawes, R.P., D.K. Byun, E.B. Brown, **K.S. Madden**. 2015. Psychosocial stress suppresses tumor progression in a murine model of spontaneous, metastatic breast cancer. Annual Psychoneuroimmunology Research Society Scientific Meeting, Seattle, WA.

Madden, **K.S.,** Dawes, R.P., D.K. Byun, E.B. Brown. 2015. Sympathetic nervous system modulation of tumor fibrillar collagen as detected by multiphoton second harmonic generation. University of Rochester Immune Imaging Symposium. November 7, 2015.

PUBLICATIONS

Szpunar, M.J., E.K. Belcher, R.P. Dawes, **K.S. Madden**. 2015. Sympathetic innervation, norepinephrine content, and norepinephrine turnover in orthotopic and spontaneous models of breast cancer. Brain Behavior and Immunity, (http://www.sciencedirect.com/science/article/pii/S0889159115300775)

No website, technology, inventions, patent applications, licenses, or other products to report.

7. PARTICIPANTS & OTHER COLLABORATING ORGANIZATIONS:

Individuals who have worked on the project:

NAME: Kelley S. Madden, PhD
Project role: PI
Researcher identifier:?
Nearest person month worked: 6
Contribution to project: Dr. Madden has planned and designed all experiments. She has assisted with the execution of these experiments. She has analyzed all results.

NAME: Daniel Byun
Project Role: Technician
Researcher Identifier: ?
Nearest person month: 10
Contribution to project: Mr. Byun has executed all aspects of the *in vivo* experiments. He has also assisted with data analysis.

NAME: Eugenia Zeng
Project Role: Undergraduate Student
Researcher Identifier: ?
Nearest person month: 1
Contribution to project: Eugenia executed all experiments isolating tumor associated fibroblasts

NAME: Seth Perry, PhD
Project Role: co-investigator
Researcher identifier: ?
Nearest person month: 1
Contribution to project: Assisted with isolation of tumor associated fibroblasts and with SHG image analysis.

No change in the active support of the PI or senior/key personnel since the last reporting period.

No other organizations were involved as partners.

APPENDICES: None